nature geoscience

LETTERS

PUBLISHED ONLINE: 6 MAY 2012 | DOI: 10.1038/NGEO1460

# Regional atmospheric circulation shifts induced by a grand solar minimum

Celia Martin-Puertas[1]*, Katja Matthes[2,3], Achim Brauer[1], Raimund Muscheler[4], Felicitas Hansen[2,5], Christof Petrick[2,3], Ala Aldahan[6,7], Göran Possnert[6] and Bas van Geel[8]

**Large changes in solar ultraviolet radiation can indirectly affect climate[1] by inducing atmospheric changes. Specifically, it has been suggested that centennial-scale climate variability during the Holocene epoch was controlled by the Sun[2,3]. However, the amplitude of solar forcing is small when compared with the climatic effects and, without reliable data sets, it is unclear which feedback mechanisms could have amplified the forcing. Here we analyse annually laminated sediments of Lake Meerfelder Maar, Germany, to derive variations in wind strength and the rate of $^{10}$Be accumulation, a proxy for solar activity, from 3,300 to 2,000 years before present. We find a sharp increase in windiness and cosmogenic $^{10}$Be deposition 2,759 ± 39 varve years before present and a reduction in both entities 199 ± 9 annual layers later. We infer that the atmospheric circulation reacted abruptly and in phase with the solar minimum. A shift in atmospheric circulation in response to changes in solar activity is broadly consistent with atmospheric circulation patterns in long-term climate model simulations, and in reanalysis data that assimilate observations from recent solar minima into a climate model. We conclude that changes in atmospheric circulation amplified the solar signal and caused abrupt climate change about 2,800 years ago, coincident with a grand solar minimum.**

The hypothesis of solar-induced centennial to decadal climate changes during the Holocene epoch suggests feedback mechanisms in the climate system amplifying even small solar variations[2–4]. A major climate shift during the Late Holocene was evidenced as a cooling and increased humidity in the North Atlantic–European region at around 2,800 calendar years before present (cal yr BP, 'present' being AD 1950) coinciding with the biostratigraphic transition from the sub-boreal to the sub-Atlantic period[5], and associated with low solar radiation[2]. A less active Sun implies high cosmogenic radionuclide production rates in the atmosphere related to weaker shielding against galactic cosmic ray fluxes; thus, the steep increase in $^{14}$C content of the atmosphere from 2, 800–2, 650 cal yr BP (ref. 6) and the rise in the cosmogenic radionuclide $^{10}$Be flux archived in Greenland ice cores[7] both point to a long-term (centennial) solar minimum from about 2,750–2,550 cal yr BP known as the Homeric minimum[8].

At the present time, observations of changes in the atmospheric and climate parameters seem to respond to the 11-year sunspot solar cycle[1]. Satellite-based measurements of total solar irradiance show that mean variations during solar cycles do not exceed 0.2 W m$^{-2}$ (∼0.1% of the total solar energy)[9]; however, relatively large variations of 5–8% have been reported in the ultraviolet[10]. These significant shifts at the 200–300 nm part of the solar emission spectrum can have significant effects on heating and ozone chemistry in the middle atmosphere, can induce indirect dynamical effects in the atmosphere down to the Earth's surface and could hence affect climate through the so-called 'top-down' mechanism[1]. This acts through disturbances of the stratospheric polar vortex that propagate by means of wave–mean flow interactions downwards, influence the tropospheric jet streams, which are connected to the Arctic Oscillation/North Atlantic Oscillation at Northern Hemisphere mid-latitudes and affect European winter variability[11,12]. Other mechanisms for solar influence on climate concern the role of energetic particles from the Sun or galactic cosmic rays, but they are energetically smaller and their climate impact is much less understood than the mechanisms connected to electromagnetic radiation[1].

Examining palaeoclimate variability for signs of 'top-down' mechanisms involved in long-term solar fluctuations requires very accurate climate reconstructions with very accurate dating to reduce uncertainties of solar-climate phasing and highly resolved palaeoclimate proxies not only for past temperatures and precipitation but also for other climate parameters such as wind strength. To match this challenge, we present unique information from a wind-sensitive varve thickness record and solar-modulated sediment $^{10}$Be accumulation rates, both connected to the same chronology of the annually laminated sediments from the Lake Meerfelder Maar (MFM); and also combine proxy data with long-term climate model simulations under natural forcings. The results will allow a precise assessment of the Homeric climate oscillation for central Europe in terms of timing, duration and abruptness, and provide a better picture of the atmospheric circulation at that time.

MFM, located in central-western Europe (50°6′ N, 6°45′ E; Fig. 1a), provides a seasonally resolved record since the onset of the Lateglacial interstadial (11.2 m length), sensitive of changes in the North Atlantic climate system[13]. In this study, we focus on the 3,300–2,000 cal yr BP interval that includes the 'Homeric climate oscillation' and base our interpretation on two annually resolved environmental indicators—varve structure and thickness considered as a proxy for seasonal lake water circulation; and titanium (Ti) variability as an indicator of allochthonous sediment

[1]Helmholtz Centre Potsdam, GFZ German Research Centre for Geosciences, Section 5.2 Climate Dynamics and Landscape Evolution, Telegrafenberg D-14473, Potsdam, Germany, [2]Helmholtz Centre Potsdam, GFZ German Research Centre for Geosciences, Section 1.3 Earth System Modelling, Telegrafenberg D-14473, Potsdam, Germany, [3]Helmholtz Centre for Ocean Research Kiel (GEOMAR), Duesternbrooker Weg 20, 24105 Kiel, Germany, [4]Department of Earth and Ecosystem Sciences, Lund University, Sölvegatan 12, SE-223 62 Lund, Sweden, [5]Freie Universität Berlin, Institut für Meteorologie, Carl-Heinrich-Becker Weg 6-10, 12165 Berlin, Germany, [6]Department of Earth Science and Tandem Laboratory, Uppsala University, SE-752 36 and SE-751 21 Uppsala, Sweden, [7]Geology Department, United Arab Emirates University, 17551 Al Ain, UAE, [8]Institute for Biodiversity and Ecosystem Dynamics, University of Amsterdam, Science Park 904, 1098 XH Amsterdam, The Netherlands. *e-mail: celia@gfz-potsdam.de.



© 2012 Macmillan Publishers Limited. All rights reserved.

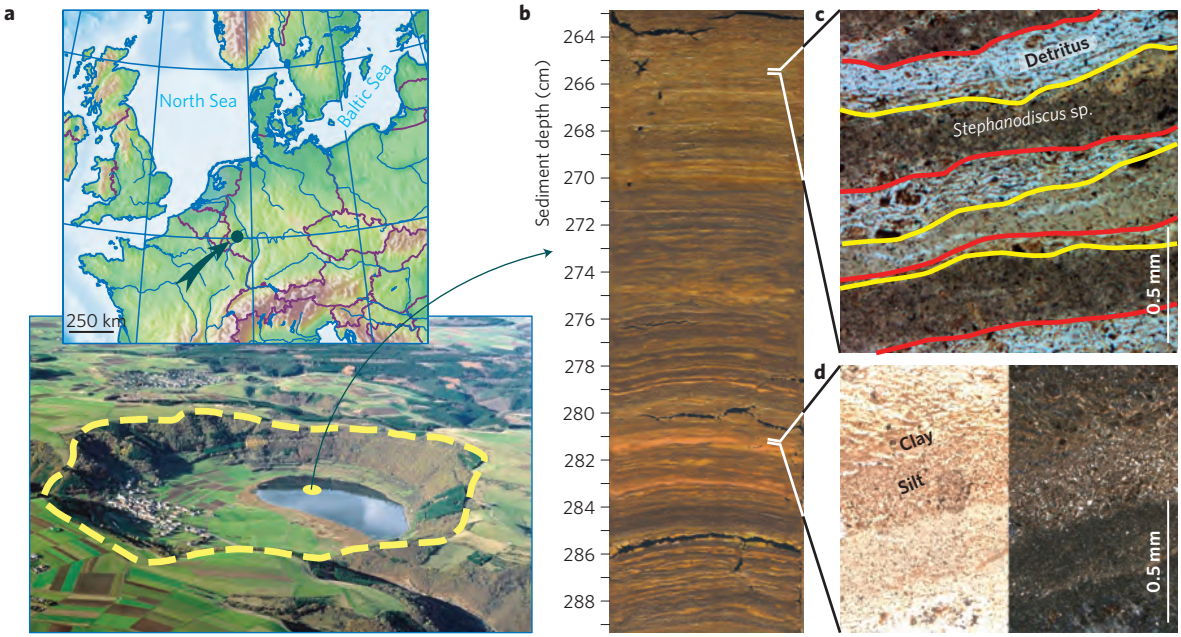


**Figure 1 | Lake Meerfelder Maar (MFM). a**, Location and aerial photo of the lake catchment. The dashed line indicates the maar crater border. The yellow dot shows the coring site in the deeper part of the lake (18 m; photo from Tourist Information Manderscheid). **b**, Core photo showing a section (263–289 cm depth) of the 3,300–2,000 cal yr BP sedimentary sequence. **c**, Photomicrographs of MFM sediments; ×5 microscope image (normal light) showing varves composed of diatom bloom (*Stephanodiscus* sp.) and detritus sub-layer. **d**, ×10 microscope image using normal (left) and polarized (right) light of a discrete graded detrital layer (KL2).

influx from the basaltic catchment—and one solar proxy as reflected by lake sediment $^{10}$Be accumulation rate.

The MFM varve chronology spans from about 1,500 to 14,200 cal yr BP. It is a floating chronology because the upper sediments are poorly laminated owing to strong human impact in the catchment. The chronology has been anchored to the absolute timescale by means of tephrochronology and radiocarbon dating[14]. For the study interval, the age model has been complemented with new parallel varve counts (estimated counting error <1%) and five additional radiocarbon dates (Supplementary Information). The 3,300–2,000 cal yr BP interval is composed of diatomaceous varves with high organic carbon contents (7.5–24%) and occasional detrital layers (~2 mm thick; Fig. 1b). Varves consist of couplets of a light laminae composed of planktonic diatom frustules (*Stephanodiscus* sp.) reflecting the early spring diatom bloom after lake ice break-up and a dark sub-layer of predominantly organic detritus deposited during the rest of the year before the winter ice cover (Fig. 1c); discrete detrital layers are graded indicating events of runoff (Fig. 1d).

The most significant feature of the studied varve sequence is the occurrence of a twofold increase in the average varve thickness (1.35 mm per varve) starting at 2,759 ± 39 varve yr BP and spanning 199 ± 9 years (Supplementary Information); with a significantly enhanced inter-annual variability (0.2–3.7 mm; Fig. 2a). Thickness increases abruptly within eight years, caused by intensified monospecific diatom blooms and higher reworked littoral diatom content deposited in the dark sub-layer. The end of the thicker varves interval is marked by a sharp fall of the mean thickness at 2,560 ± 48 varve yr BP. Intensification of the *Stephanodiscus* sp. bloom requires phosphorous (P) availability, which is its limiting nutrient. A possible major contribution of P flux from the catchment can be ruled out because there is no evidence of higher allochthonous sediment influx 3(Ti) until 70 varve years after the change (Fig. 2a). Furthermore, the increase in detrital layers occurs around 100 varve years later (not shown). In contrast, the occurrence of thicker varves could be ascribed to strengthened winds in the season of spring ice break-up generating stronger water circulation and upward mixing of nutrients from the bottom water to the photic zone (phosphate recycling), and intensified wave activity at the shoreline acting as an erosive agent (Supplementary Information). The interpretation of wind-induced diatom blooms is further supported by the reported sensitivity of MFM sediments to changes in wind systems during earlier climate periods[13]. Moreover, the highest values of $^{10}$Be flux occur during the windy interval (Supplementary Information). The agreement of the atmospheric $^{14}$C production rate as inferred from tree ring $\Delta^{14}$C (ref. 15), the GRIP $^{10}$Be flux in ice core[7] and the MFM sediment $^{10}$Be flux supports the link to solar activity (Fig. 2b). Possible alternative explanations such as climate influence on the $^{10}$Be deposition or carbon-cycle influences on the atmospheric $^{14}$C concentrations are very unlikely to yield a synchronous signal with similar amplitude. Changes in the geomagnetic field have also been excluded because there are no records that could explain the large increases in the $^{10}$Be and $^{14}$C rate during this period.

The signature of climate change in the wind-proxy record of MFM is supported by the coincidence with the Homeric climate oscillation in Europe, which was characterized by a cooling and a shift towards more humid conditions[5,16] (Fig. 2c). In addition, the link to solar activity as reflected by cosmogenic radionuclides indicates that windy conditions prevailed while the solar irradiance was low (Fig. 2a,b). As the wind signal recorded in the MFM record corresponds to the late winter–early spring (diatom bloom), we infer a very rapid (less than a decade) and direct linkage between the long-term solar minimum and intensification of the regional tropospheric circulation during this season.

To support these findings, we investigate the climate response during recent 11-year solar cycle minima in coupled chemistry–climate model simulations (Fig. 3; Methods) as well as in reanalysis data (Fig. 4; Methods) during the same seasonal window (February to April) and compare it with the response found in proxy data for the Homeric minimum. The modelled sea level pressure (Fig. 3a) shows positive pressure changes over Iceland and negative changes in the subtropics during solar minima as compared with



© 2012 Macmillan Publishers Limited. All rights reserved.

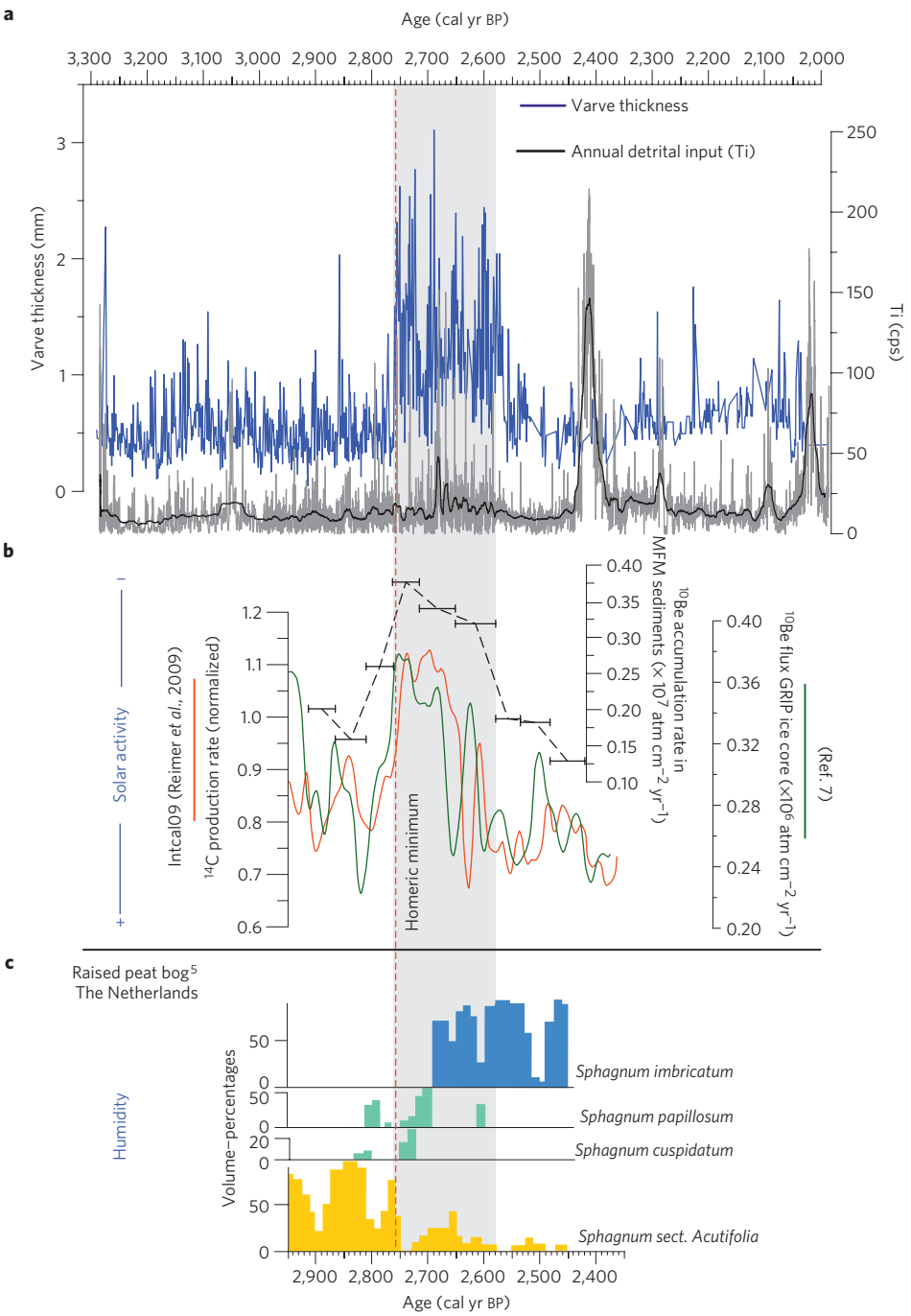


**Figure 2 | MFM proxy data. a**, Varve thickness variability (blue) and titanium (Ti) variability (grey) from 3,300 to 2,000 cal yr BP; Ti intensity is expressed in counts per second (cps); the dark grey line indicates smoothing by 100-data running average. **b**, Proxies for solar activity: $^{10}$Be accumulation rate in MFM sediments expressed in flux units (black), the error bars show the age uncertainty for each sediment sample; normalized $^{14}$C production rate[15] (red); and $^{10}$Be flux from the GRIP ice core[7] (green). **c**, Raised bog-based humidity proxy for the Netherlands interpreted showing evidence for the 'Homeric climate oscillation' in western Europe[5].

the long-term mean. This reduced pressure gradient resembles a negative phase of the North Atlantic Oscillation and results in lower temperatures over northern and middle Europe and higher temperatures over Greenland (Fig. 3b). The North Atlantic storm tracks are shifted further south with a maximum over the Mediterranean (Fig. 3d) and thus carry more moist air to central and southern Europe as seen in enhanced precipitation (Fig. 3c). Focusing on the anomalies for the MFM location confirms the proxy-data reconstruction with an increase in the upper tropospheric winds (about 1 m s$^{-1}$), as well as slightly cooler conditions (about 0.5 K) and an increase in precipitation (about 4 mm) during recent solar minimum conditions. As these modelled anomalies occur in late winter to early spring and have a direct connection to stratospheric circulation changes under natural forcings alone (Supplementary Fig. S5 and Methods), we suggest a similar 'top-down' mechanism working on longer timescales triggering climate change at mid-latitudes. Moreover, our interpretation of the palaeodata as well as the results of the idealized climate model experiments can be further supported by reanalysis data of the recent past (Fig. 4). Qualitatively similar



© 2012 Macmillan Publishers Limited. All rights reserved.

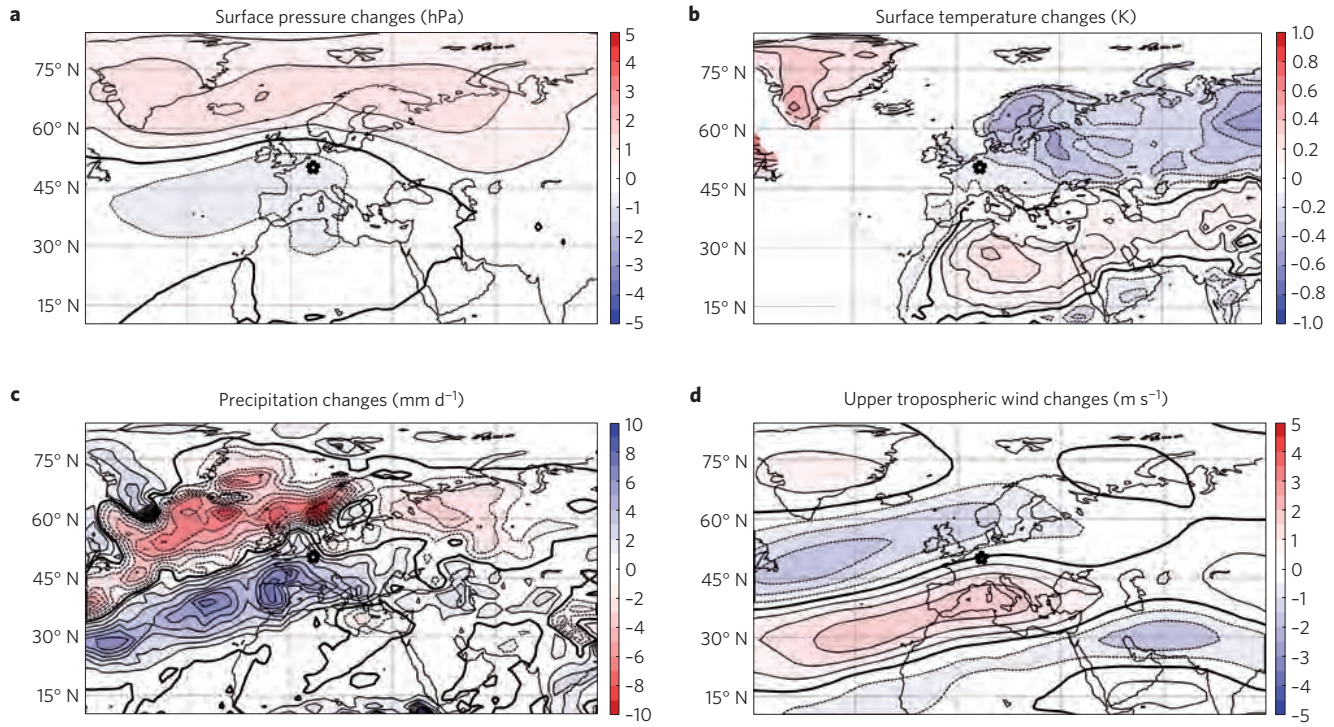


**Figure 3 | Modelled solar signal. a–d**, Differences between solar minimum (f10.7 < 90 solar flux units) and the climatological mean of all years averaged from February to April for the sea-level pressure in hectopascal (hPa; **a**), the surface temperature in Kelvin (K; **b**), precipitation in millimetres per day (mm $d^{-1}$; **c**) and upper tropospheric wind in metres per second (m $s^{-1}$; **d**) at 500 hPa for Europe from a 140-year coupled chemistry–climate model simulation.

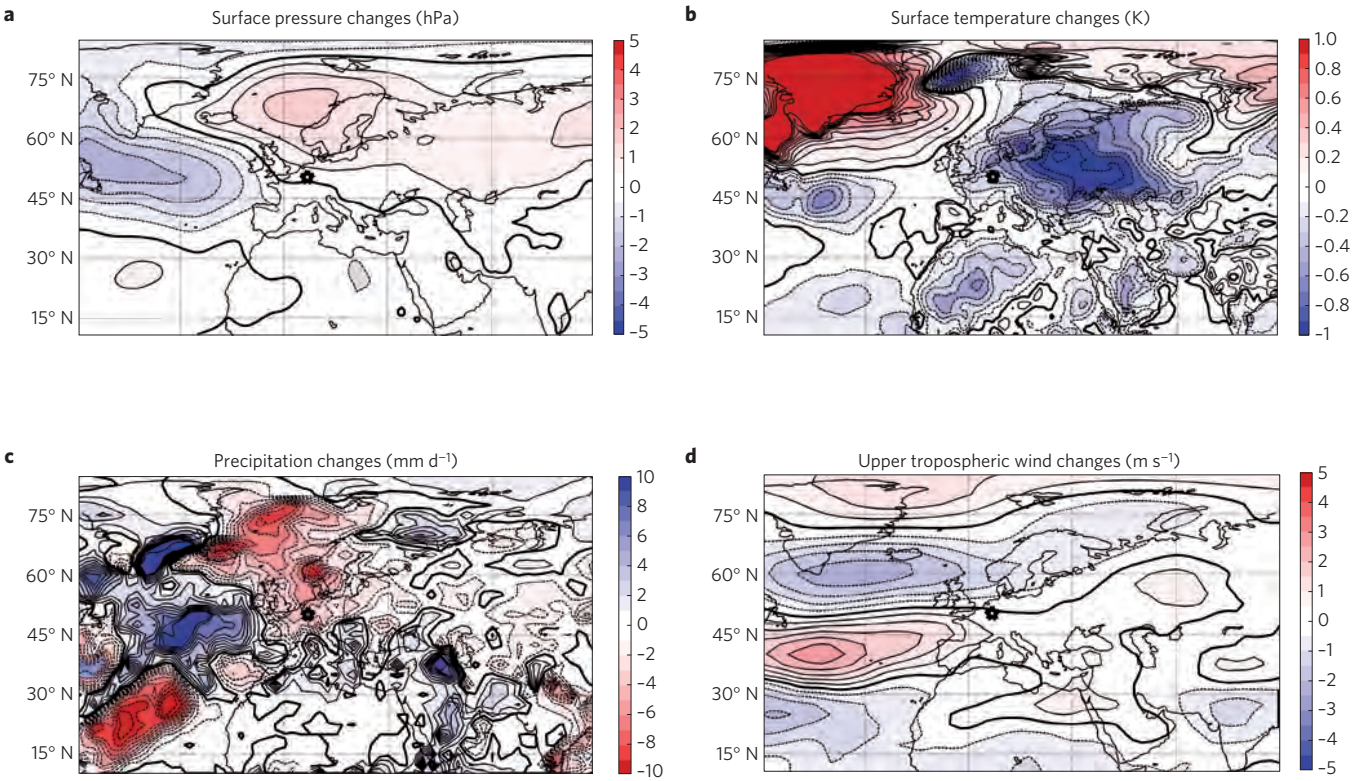


**Figure 4 | ERA-40/ERA-Interim reanalyses[22].** The same as in Fig. 3.

pressure, temperature, winds and precipitation changes to those in the climate model occur over MFM during recent solar minimum conditions in the reanalysis data. However, slight differences when compared with the climate model response occur that are related to the slightly different shape of the absolute pressure and wind fields (not shown).



© 2012 Macmillan Publishers Limited. All rights reserved.

The model study as well as the reanalysis data can be used to estimate the climate response during periods of low solar activity. However, a direct comparison to the Homeric minimum, which was a very deep and persistent minimum with very different orbital parameters when compared with recent solar minima and probably a larger climate response, is not possible. This study shows unique high-resolution lake sediment data for the Homeric climate oscillation 2,800 years ago providing synchronous solar minimum and windy conditions during late winter to early spring in western Europe. On the basis of idealized climate model experiments with resolved stratosphere as well as reanalysis data, we propose a solar-induced 'top-down' mechanisms working on the centennial timescale. This is in agreement with a recent study[17], in which the importance of solar ultraviolet forcing on Northern Hemisphere winter climate (December to February) is highlighted. Despite limitation in the resolution of the sediment data allowing to specify seasons but not individual months and model experiments not specifically designed for the time interval of the Homeric minimum, the combination of both proxy data and climate models highlights a possible role of the solar forcing not only during the winter but also on the early spring climate over the European Atlantic sector.

## Methods

**Lake sediments.** Microfacies were studied on overlapping thin sections of 10 cm of length. Ti intensities were directly measured on impregnated sediment blocks used for thin-section preparation[18] with an EAGLE III BKA spectrometer at 100 and 52 μm resolutions (10–60 data points per varve depending on annual sedimentation rate). $^{10}$Be was extracted from about 0.4 to 1 g of sediment sample (∼60 varves per sample). Sample preparation and measurements were carried out at the Uppsala Tandem Laboratory AMS facility[19]. $^{10}$Be accumulation rate ($a$) was calculated as: $a(\text{atoms cm}^{-2}\,\text{yr}^{-1}) = c\,(\text{atoms g}^{-1}) \times SAR(\text{cm}^{-2}\,\text{yr}^{-1})$, where $c$ is concentration and $SAR$ is sediment accumulation rate.

**Climate model simulations.** We use NCAR's Community Earth System Model (CESM), a coupled chemistry–climate model with the Whole Atmosphere Community Climate Model (WACCM) atmospheric component (2.5° × 1.9° horizontal resolution and 66 vertical levels up to 140 km height), an interactive ocean (horizontal curvi-linear grid of approximately 1° with 60 vertical layers) and land and sea ice modules[20]. A 140-year simulation (1955–2100) under natural forcings alone (spectrally resolved solar irradiance changes from the far-ultraviolet to the near-infrared[9], externally prescribed quasi-biennial oscillation[21], no volcanoes, and 1960 levels of greenhouse-gas emissions and ozone-depleting substances) using time-varying forcings is performed.

**Reanalysis data.** ERA-40/ERA-Interim reanalysis data[22] from 1958 to 2011 are separated into solar maximum and solar minimum years according to the f10.7 cm solar radio flux.

Received 24 January 2012; accepted 2 April 2012; published online 6 May 2012

## References


1. Gray, L. J. *et al.* Solar influences on climate. *Rev. Geophys.* **48,** RG4001 (2010).
2. Van Geel, B. *et al.* The role of solar forcing upon climate change. *Quater. Sci. Rev.* **18,** 331–338 (1999).
3. Magny, M. Solar influences on Holocene climatic changes illustrated by correlations between past lake-level fluctuations and the atmospheric $^{14}$C record. *Quat. Res.* **40,** 1–9 (1993).
4. Shindell, D. T., Schmidt, G. A., Mann, M. E., Rind, D. & Waple, A. Solar forcing of regional climate change during the Maunder Minimum. *Science* **294,** 2149–2152 (2004).
5. Van Geel, B., Buurman, J. & Waterbolk, H. T. Archaelogical and palaeoecological indications of an abrupt climate change in The Netherlands, and evidence for climatological teleconnections around 2650 BP. *J. Quat. Sci.* **11,** 451–460 (1996).
6. Reimer, P. J. *et al.* Intcal09 and Marine09 radiocarbon age calibration curves, 0-50,000 years cal BP. *Radiocarbon* **51,** 1111–1150 (2009).
7. Vonmoos, M., Beer, J. & Muscheler, R. Large variations in Holocene solar activity: Constraints from $^{10}$Be in Greenland Ice Core Project ice core. *J. Geophys. Res.* **111,** A10105 (2006).
8. Stuiver, M. & Kra, R. Calibration issue. *Radiocarbon* **28,** 805–1030 (1986).
9. Lean, J., Rottman, G., Harder, J. & Kopp, G. SORCE contributions to new understanding of global change and solar variability. *Sol. Phys.* **230,** 27–53 (2005).
10. Lean, J. L. *et al.* Detection and parameterisation of variations in solar mid- and near-ultraviolet radiation (200–400 nm). *J. Geophys. Res.* **102,** 29939–29956 (1997).
11. Kuroda, Y. & Kodera, K. Role of the polar-night jet oscillation on the formation of the arctic oscillation in the northern hemisphere winter. *J. Geophys. Res.* **109,** D11112 (2004).
12. Wooling, T., Lockwood, M., Masato, G., Bell, C. & Gray, L. Enhanced signature of solar variability in Eurasian winter climate. *Geophys. Res. Lett.* **37,** L20805 (2010).
13. Brauer, A., Haug, G. H., Dulski, P., Sigman, D. M. & Negendank, J. F. W. An abrupt wind shift in western Europe at the onset of the Younger Dryas cold period. *Nature Geosci.* **1,** 520–523 (2008).
14. Brauer, A., Endres, C., Zolitschka, B. & Negendank, J. F. W. AMS radiocarbon and varve chronology from the annually laminated sediments record of lake Meerfelder Maar, Germany. *Radiocarbon* **42,** 355–368 (2000).
15. Muscheler, R., Beer, J., Kubik, P. W. & Synal, H-A. Geomagnetic field intensity during the last 60,000 years based on $^{10}$Be & $^{36}$Cl from the Summit ice cores and $^{14}$C. *Quater. Scie. Rev.* **24,** 1849–1860 (2005).
16. Holzhauser, H., Magny, M. & Zumbühl, H. J. Glacier and lake-level variations in west-central Europe over the last 3500 years. *Holocene* **15,** 789–801 (2005).
17. Ineson, *et al.* Solar forcing of winter climate variability in the Northern Hemisphere. *Nature Geosci.* **4,** 753–757 (2011).
18. Brauer, A., Dulski, P., Mangili, C., Mingram, J. & Liu, J. The potential of varves in high-resolution paleolimnological studies. *PAGES News* **17,** 96–98 (2009).
19. Berggren, A. M., Possnert, G. & Aldahan, A. Enhanced beam currents with co-precipitated niobium as a matrix for AMS measurements of $^{10}$Be. *Nucl. Instrum. Methods* **268,** 795–798 (2010).
20. Gent, P. R. *et al.* The community climate system model version 4. *J. Clim.* **24,** 4973–4991 (2011).
21. Matthes, K. *et al.* Role of the QBO in modulating the influence of the 11-year solar cycle on the atmosphere using constant forcings. *J. Geophys. Res.* **115,** D18110 (2010).
22. Uppala, S. M. *et al.* The ERA-40 re-analysis. *Q. J. R. Meteorol. Soc.* **131,** 2691–3012 (2005).


## Acknowledgements

C.M-P. acknowledges financial support from the Alexander von Humboldt Foundation. The work of K.M., F.H. and C.P. has been carried out within the Helmholtz University Young Investigators Group NATHAN financially supported by the Helmholtz-Association through the President's Initiative and Networking Fund, the GFZ Potsdam and by FU Berlin and now transferred to the Helmholtz Centre for Ocean Research Kiel (GEOMAR). The model calculations have been performed at the Deutsche Klimarechenzentrum (DKRZ) Hamburg. R.M. is supported by the Swedish Academy of Sciences (KVA) through the Knut and Alice Wallenberg Foundation. This study is a contribution to the Helmholtz-Association climate initiative REKLIM (Topic 8 'Rapid Climate Change from Proxy Data'). The authors thank N. Dräger and F. Ott for varve counting, A. Heinrich for the graphical support and S. Engels for valuable comments.

## Author contributions

C.M-P. led the writing of the manuscript and was responsible for sediment core data analyses. A.B. led the coring campaign and contributed to varve analyses and chronology. C.M-P., A.B., R.M. and B.v.G. jointly interpreted the proxy data. K.M. was responsible for climate model simulations. K.M., F.H. and C.P. performed the climate model simulations and interpreted the reanalysis data. A.A. and G.P. measured the $^{10}$Be samples. All authors contributed to the discussion and the writing of the final manuscript. A.B. and C.M-P. conceived and designed the study.

## Additional information

The authors declare no competing financial interests. Supplementary information accompanies this paper on www.nature.com/naturegeoscience. Reprints and permissions information is available online at www.nature.com/reprints. Correspondence and requests for materials should be addressed to C.M-P.



© 2012 Macmillan Publishers Limited. All rights reserved.